Bull. Chem. Soc. Jpn., ***68***, *2305—2311(1995)*

Dissolution Behavior of Optical Isomers of *fac*-Tris(aniono)cobalt(III) of Some α-Amino Acids in Water

Yasuki Yoshimura

Laboratory of Chemistry, Faculty of Humanities and Social Sciences, Iwate University, Ueda, Morioka 020

(Received March 10, 1995)

fac-Tris(aniono)cobalt(III) of D-alanine, D-valine, D-leucine, L- and D-prolines, and L- and D-serines was synthesized, and the separation of the diastereoisomers of these chelates was attempted. The solubilities of these isomers in water were determined over the temperature range of 5 to 55 °C. The thermodynamic parameters of solution at 25 °C, such as the free energy (ΔG_s°), enthalpy (ΔH_s°), and entropy (ΔS_s°), were estimated from the temperature dependence of the solubilities. Also, the dissolution behavior of these chelate in water was considered in terms of these thermodynamic parameters. Plot of ΔH_s° against $T\Delta S_s^\circ$ gave separate correlation lines for the groups comprising less soluble chelates and more soluble chelates. An increase in the solubility within the respective groups was caused by an increase in $T\Delta S_s^\circ$. Both ΔH_s° and $T\Delta S_s^\circ$ for the chelates of less hydrophobic glycine and serine were larger than those for the chelates of more hydrophobic amino acids.

In a preceding study,[1] the dissolution behavior of the *fac*-tris(aniono)cobalt(III) of L-alanine (L-alaH), L-2-aminobutanoic acid (L-ambtH), L-valine (L-valH), and L-leucine (L-leuH) in water was examined in order to obtain fundamental information for interpreting the properties of metal–protein complexes. A systematic interpretation of the dissolution behavior of amino acid chelates requires the examination of a wide variety of amino acid chelates.

The optical isomers, (+)- and (−)-isomers of *fac*-tris(L-amino acidato)cobalt(III) (*fac*-[Co(L-amino acidato)$_3$]), are diastereoisomers, and antipodes of these isomers are the (−)- and (+)-isomers of the corresponding *fac*-tris(D-amino acidato)cobalt(III) (*fac*-[Co(D-amino acidato)$_3$), respectively. In this paper (+) and (−) represent dextrorotatory and levorotatory at 589 nm, respectively. The above fact suggests that the dissolution behavior of *fac*-[Co(D-amino acidato)$_3$] in water should exhibit the same features as do those found for *fac*-[Co(L-amino acidato)$_3$]. It would be noteworthy to confirm this suggestion by experimental results.

Thus, in the present work the (+)- and (−)-isomers of *fac*-tris(aniono)cobalt(III) of D-alaH, D-valH, and D-leuH were isolated, and the dissolution behavior of these chelates in water examined on the basis of the thermodynamic parameters of solution estimated from the temperature dependence of their solubilities. In addition, the solubilities of the (+)- and (−)-isomers of *fac*-tris(aniono)cobalt(III) of L- and D-prolines (L- and D-proH), which are cyclic amino acids, were also determined with the view to examine any influence of the cyclized side chain on the dissolution behavior of these chelates.

In the preceding study,[1] a procedure for estimating the thermodynamic parameters of hydrophobic hydration was proposed. In this procedure it is postulated on the basis of the temperature dependence of the solubility for *fac*-tris(glycinato)cobalt(III) (*fac*-[Co(gly)$_3$])[2] that a linear temperature dependence of the solubility implies dissolution without hydrophobic hydration. In order to clarify the feature of dissolution without hydrophobic hydration, *fac*-tris(aniono)cobalt(III) of L- and D-serines (L- and D-serH), in which hydrophobic $-CH_3$ groups of L- and D-alaH are replaced by hydrophilic $-CH_2OH$ groups, was synthesized, and the temperature dependence of their solubilities compared with that of *fac*-tris(L- or D-alaninato)cobalt(III) (*fac*-[Co(L-ala)$_3$] and *fac*-[Co(D-ala)$_3$]).

Furthermore, the solubility of L-phenylalanine (L-phalaH) was also determined, and its thermodynamic parameters of solution compared with those of the amino acid chelates.

Experimental

The syntheses of *fac*-tris(aniono)cobalt(III) of D-alaH, D-valH, D-leuH, and L-serH (*fac*-[Co(D-val)$_3$], *fac*-[Co(D-leu)$_3$], and *fac*-[Co(L-ser)$_3$]) and the separation of their (+)- and (−)-isomers were carried out in the same manner as previously reported,[1] except for the separation of *fac*-(+)-[Co(D-ala)$_3$] and *fac*-(−)-[Co(L-ser)$_3$] (see below). *fac*-Tris(L- or D-prolinato)cobalt(III) (*fac*-[Co(L-pro)$_3$] and *fac*-[Co(D-pro)$_3$]) was synthesized and separated into (+)- and (−)-isomers by using a procedure reported in the literature.[3]

fac-Tris(D-serinato)cobalt(III) (*fac*-[Co(D-ser)$_3$]) was synthesized in a manner similar to that for *fac*-[Co(pro)$_3$]. Separation into the (+)- and (−)-isomers was effected as follows: After the reaction mixture of D-serH with tris(carbonato)-

cobaltate(III) ion was concentrated to about 100 cm^3, a red solid (*fac*-(−)-[Co(D-ser)$_3$]) was removed by filtration; the filtrate was passed separately through a cation-exchange resin in the hydrogen ion form and an anion-exchange resin in the hydroxide form; after the deionized eluent was concentrated to about 50 cm^3, a purple solid (*mer*-(−)-[Co(D-ser)$_3$]) was removed by filtration; the filtrate was chromatographed on an alumina column (50 cm high and 3.5 cm in diameter) and eluted with water; a large quantity of a purple band (mainly *mer*-(+)-[Co(D-ser)$_3$]) separated first, followed by a red band containing *fac*-(+)-[Co(D-ser)$_3$]; the second eluent was concentrated to about 10 cm^3 and crystallized by adding ethanol. The separation of *fac*-(+)-[Co(D-ala)$_3$] and *fac*-(−)-[Co(L-ser)$_3$] was also effected in a similar manner.

For chelates other than *fac*-[Co(D-val)$_3$], for which only the (−)-isomer could be isolated, both the (+)- and (−)-isomers could be obtained. Each isomer was identified by measuring the CD spectrum of its solution in 60% sulfuric acid or in water.

In this study, the solubility of freshly prepared *fac*-(−)-[Co(L-ala)$_3$] was redetermined for the reason to be described subsequently. The preparation was carried out by using the same procedure as that for *fac*-(+)-[Co(D-ser)$_3$].

The solubility was measured by using the same apparatus as previously used.[4] The detailed procedure for the solubility measurement was described in the preceding paper.[1] The solubility in mol kg^{-1} (S_m) was obtained by calculating the number of the chelate molecules or L-phalaH molecules in an aliquot of the saturated solution based on the concentration of the chelate or L-phalaH in the working solution prepared by diluting the above-mentioned aliquot. The above-mentioned concentration was determined spectrophotometrically.

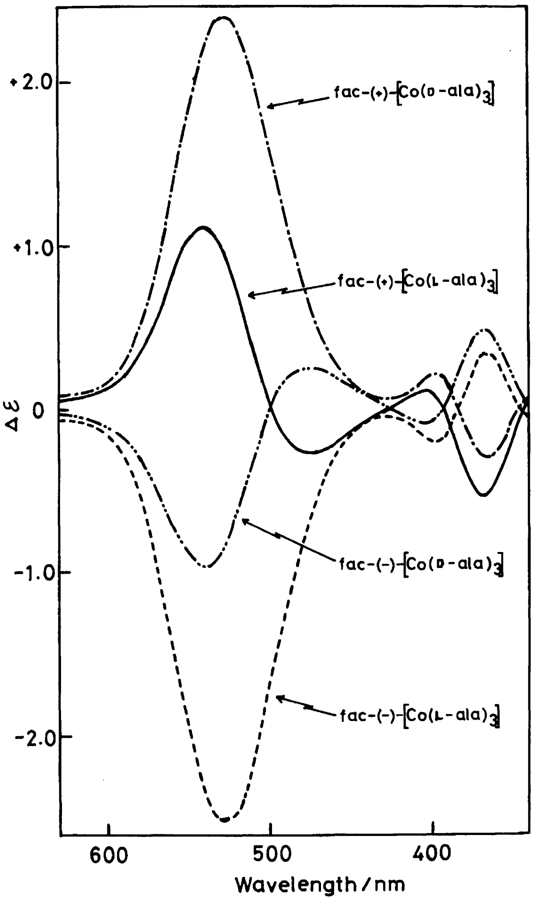

Fig. 1. CD spectra of the optical isomers of *fac*-[Co(D-ala)$_3$] and *fac*-[Co(L-ala)$_3$].

Results

As a typical example, the CD spectra for the (+)- and (−)-isomers of *fac*-[Co(D-ala)$_3$] are shown in Fig. 1, where the CD spectra for both isomers of *fac*-[Co(L-ala)$_3$] are also given for a comparison. The comparison of these CD spectra shows that the antipodes of the (+)- and (−)-isomers of *fac*-[Co(D-ala)$_3$] are the (−)- and (+)-isomers of *fac*-[Co(L-ala)$_3$], respectively. The CD spectra of the other chelates also resulted in the same conclusion.

The S_m values in water are listed in Table 1 for *fac*-[Co(D-ala)$_3$], *fac*-[Co(D-leu)$_3$], and *fac*-(−)-[Co(L-ala)$_3$], in Table 2 for *fac*-[Co(L-ser)$_3$], *fac*-[Co(L-pro)$_3$], and *fac*-(−)-[Co(D-val)$_3$], and in Table 3 for *fac*-[Co(D-ser)$_3$], *fac*-[Co(D-pro)$_3$], and L-phalaH. The solubility measurement was repeated at least four times at each tem-

Table 1. Solubilities (S_m) for the (−)- and (+)-Isomers of *fac*-[Co(D-ala)$_3$] and *fac*-[Co(D-leu)$_3$], and for *fac*-(−)-[Co(L-ala)$_3$] in Water[a)]

T/°C	*fac*-(−)-[Co(D-ala)$_3$] $S_m/10^{-5}$mol kg^{-1}	*fac*-(+)-[Co(D-ala)$_3$] $S_m/10^{-2}$mol kg^{-1}	*fac*-(−)-[Co(D-leu)$_3$] $S_m/10^{-6}$mol kg^{-1}	*fac*-(+)-[Co(D-leu)$_3$] $S_m/10^{-5}$mol kg^{-1}	*fac*-(−)-[Co(L-ala)$_3$][b)] $S_m/10^{-2}$mol kg^{-1}
5	1.65±0.05	4.87±0.06	4.17±0.46	1.57±0.03	5.06±0.03
10	1.74±0.02	4.82±0.02	4.56±0.26	1.46±0.01	5.05±0.03
15	1.87±0.06	4.81±0.04	4.66±0.16	1.36±0.02	4.95±0.06
20	2.07±0.06	4.83±0.03	4.89±0.12	1.31±0.02	4.91±0.04
25	2.14±0.02	4.82±0.03	5.44±0.13	1.32±0.02	4.87±0.04
30	2.20±0.03	4.91±0.02	5.60±0.05	1.33±0.01	4.86±0.01
35	2.26±0.07	4.90±0.03	5.91±0.11	1.35±0.02	4.95±0.03
40	2.50±0.07	4.91±0.06	6.09±0.20	1.39±0.02	4.95±0.06
45	2.69±0.04	4.99±0.09	7.10±0.25	1.49±0.01	5.15±0.04
50	2.85±0.05		7.98±0.33	1.65±0.03	5.27±0.06
55	3.01±0.05		9.28±0.34	1.82±0.03	

a) Errors denote 95% confidence levels. b) Redetermined in this work (see text).

Table 2. Solubilities (S_m) for the (+)- and (−)-Isomers of *fac*-[Co(L-ser)$_3$] and *fac*-[Co(L-pro)$_3$], and for *fac*-(−)-[Co(D-val)$_3$] in Water[a)]

T/°C	*fac*-(+)-[Co(L-ser)$_3$] $S_\mathrm{m}/10^{-5}\mathrm{mol\ kg^{-1}}$	*fac*-(−)-[Co(L-ser)$_3$] $S_\mathrm{m}/10^{-2}\mathrm{mol\ kg^{-1}}$	*fac*-(+)-[Co(L-pro)$_3$] $S_\mathrm{m}/10^{-5}\mathrm{mol\ kg^{-1}}$	*fac*-(−)-[Co(L-pro)$_3$] $S_\mathrm{m}/10^{-3}\mathrm{mol\ kg^{-1}}$	*fac*-(−)-[Co(D-val)$_3$] $S_\mathrm{m}/10^{-4}\mathrm{mol\ kg^{-1}}$
5	3.66±0.09	3.29±0.04	3.65±0.05	5.11±0.04	1.42±0.03
10	4.36±0.10	3.83±0.05	4.01±0.07	5.16±0.02	1.56±0.01
15	5.61±0.10	4.29±0.05	4.45±0.04	5.24±0.03	1.76±0.01
20	6.84±0.07	4.92±0.08	4.83±0.07	5.34±0.02	1.97±0.01
25	7.96±0.16	5.52±0.04	5.35±0.03	5.53±0.04	2.27±0.02
30	9.68±0.20	6.52±0.09	5.89±0.04	5.75±0.02	2.62±0.02
35	11.4±0.1		6.46±0.02	6.05±0.03	3.09±0.03
40	13.8±0.1		7.08±0.05	6.46±0.04	3.66±0.04
45	16.6±0.3		7.85±0.04	6.89±0.04	
50			8.74±0.06		
55			9.79±0.02		

a) Errors denote 95% confidence levels.

Table 3. Solubilities (S_m) for the (−)- and (+)-Isomers of *fac*-[Co(D-ser)$_3$] and *fac*-[Co(D-pro)$_3$], and for L-phalaH in Water[a)]

T/°C	*fac*-(−)-[Co(D-ser)$_3$] $S_\mathrm{m}/10^{-5}\mathrm{mol\ kg^{-1}}$	*fac*-(+)-[Co(D-ser)$_3$] $S_\mathrm{m}/10^{-2}\mathrm{mol\ kg^{-1}}$	*fac*-(−)-[Co(D-pro)$_3$] $S_\mathrm{m}/10^{-5}\mathrm{mol\ kg^{-1}}$	*fac*-(+)-[Co(D-pro)$_3$] $S_\mathrm{m}/10^{-3}\mathrm{mol\ kg^{-1}}$	L-phalaH $S_\mathrm{m}/10^{-1}\mathrm{mol\ kg^{-1}}$
5	2.61±0.03	3.24±0.04	3.70±0.03	5.26±0.04	1.21±0.01
10	3.41±0.05	3.62±0.07	4.07±0.06	5.28±0.04	1.31±0.01
15	4.24±0.06	4.08±0.06	4.36±0.02	5.25±0.05	1.39±0.01
20	5.37±0.06	4.60±0.08	4.83±0.05	5.39±0.03	1.52±0.01
25	6.59±0.10	5.34±0.03	5.28±0.05	5.57±0.07	1.65±0.01
30	8.18±0.06	6.04±0.09	5.81±0.03	5.87±0.03	1.80±0.01
35	10.2±0.1	6.66±0.08	6.44±0.06	6.19±0.04	1.97±0.01
40	12.6±0.1	7.42±0.06	7.12±0.09	6.59±0.01	2.14±0.02
45	15.2±0.2		7.98±0.03	7.09±0.03	2.29±0.01
50	17.7±0.3		8.75±0.03		2.48±0.02
55			9.83±0.06		2.71±0.01

a) Errors denote 95% confidence levels.

perature. The S_m values listed in these tables are the mean of the individual experimental values. The errors denote the deviations at the 95% confidence level, and are less than 2% in most cases. The errors for *fac*-(−)-[Co(D-leu)$_3$] are fairly large because of its low solubility.

In order to examine whether geometrical (*fac*→*mer*) or optical isomerization ((+)→(−) or (−)→(+)) occurs or not at elevated temperatures, the visible and CD spectra in the aqueous solutions of *fac*-(−)-[Co(L-ala)$_3$] and *fac*-(+)-[Co(D-pro)$_3$], whose solubilities in water are fairly large, were measured at both 25 and 50 °C (the CD spectra were measured at room temperature after standing for 5 d at 50 °C. Since standing at 50 °C had no influence on either the visible or CD spectra, the above-mentioned isomerization may be ignored even at 50 °C. Furthermore, in solubility measurements for *fac*-(+)-[Co(D-leu)$_3$] and *fac*-(+)-[Co(L-pro)$_3$], it was found that when the solution at the end of the experiment at 55 °C was allowed to attain equilibrium at 25 °C, the solubility data at 25 °C was reproducible within the experimental error. This result shows that the geometrical or optical isomerization may be neglected during the course of the solubility measurement.

In the cases of highly soluble chelates, such as *fac*-(−)-[Co(L-ser)$_3$], *fac*-(+)-[Co(D-ser)$_3$], *fac*-(−)-[Co(L-ala)$_3$], and *fac*-(+)-[Co(D-ala)$_3$], a fairly low yield of these chelates restricted the range of temperature for the solubility measurements. The solubilities of L-phalaH in Table 3 are slightly smaller than the literature values (for example, the literature value at 25 °C is 0.179 mol kg^{-1}).[5)]

The S_m values were converted to the solubilities in mole fraction (X_s), and $\ln X_\mathrm{s}$ was plotted against $1/T$. As typical examples, the solubility curves of *fac*-[Co(L-ser)$_3$] and *fac*-[Co(D-ser)$_3$] in Fig. 2, those of *fac*-[Co(D-leu)$_3$], *fac*-(−)-[Co(D-ala)$_3$], and *fac*-(+)-[Co(L-pro)$_3$] in Fig. 3, and those of *fac*-(−)-[Co(D-val)$_3$], *fac*-(+)-[Co(D-ala)$_3$], *fac*-(+)-[Co(D-pro)$_3$], and L-phalaH are shown in Fig. 4.

Since the solubilities of all the chelates studied in this work are relatively small, these saturated solutions may be regarded as being ideal dilute solutions, which are the standard states for the solutes. Thus, the standard free energy ($\Delta G_\mathrm{s}^\circ$), enthalpy ($\Delta H_\mathrm{s}^\circ$), and entropy of solution ($\Delta S_\mathrm{s}^\circ$) at 25 °C were estimated based on the temperature dependence of the solubilities in the

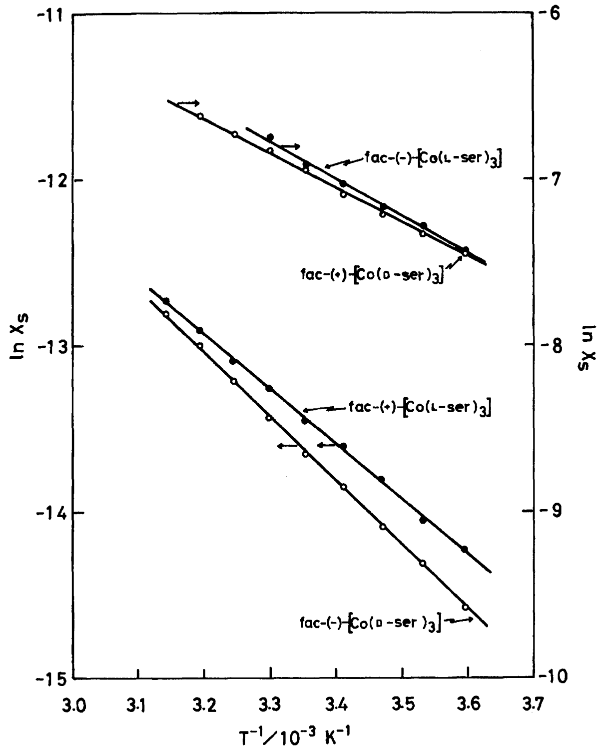

Fig. 2. Solubility curves for the (+)- and (−)-isomers of *fac*-[Co(L-ser)$_3$] and *fac*-[(D-ser)$_3$] in water depicted by plotting ln X_s against $1/T$.

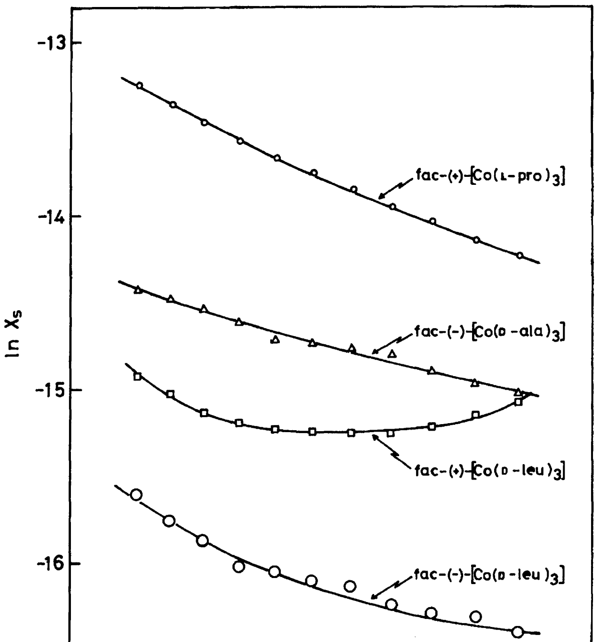

Fig. 3. Solubility curves for *fac*-(−)-[Co(D-leu)$_3$], *fac*-(+)-[Co(D-leu)$_3$], *fac*-(−)-[Co(D-ala)$_3$], and *fac*-(+)-[Co(L-pro)$_3$] in water depicted by plotting ln X_s against $1/T$.

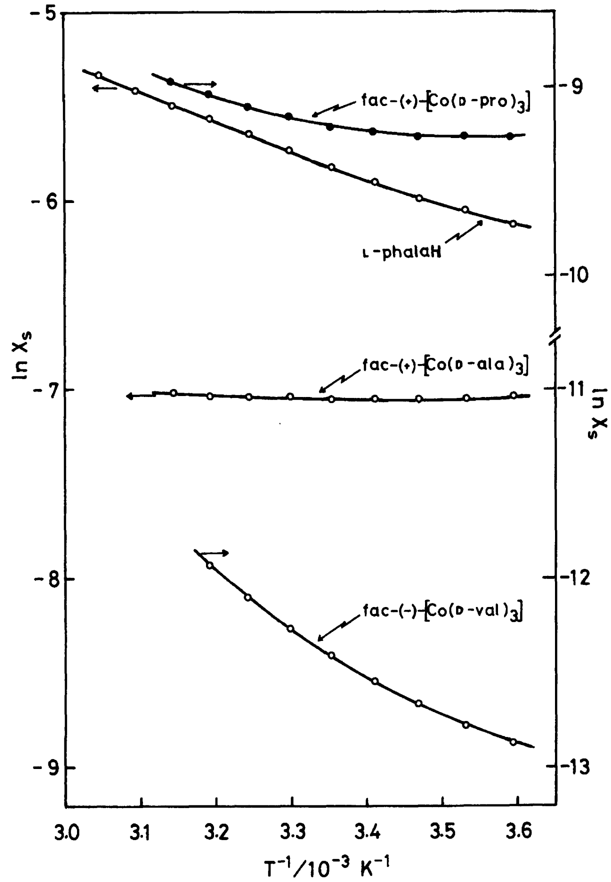

Fig. 4. Solubility curves for *fac*-(−)-[Co(D-val)$_3$], *fac*-(+)-[Co(D-pro)$_3$], *fac*-(+)-[Co(D-ala)$_3$], and L-phalaH in water depicted by plotting ln X_s against $1/T$.

same manner as previously reported.[6] The large solubility of L-phalaH seems to require an activity correction in order to estimate the standard thermodynamic parameters, though the solubility values given in Table 3 were used without any correction. These thus-estimated thermodynamic parameters are listed in Table 4.

Discussion

As shown in Figs. 2, 3, and 4, the solubility curves of *fac*-[Co(L-ser)$_3$] and *fac*-[Co(D-ser)$_3$] are practically linear, though the solubility curves of the other chelates display an upward curvature. Duke et al. have reported on the basis of heat-capacity measurements that the hydration of L-serH is essentially hydrophilic.[7] These findings support the postulation that the linear solubility curve may be regarded as being a measure of negligible hydrophobic effect. In the preceding study[1] the thermodynamic parameters of the hypothetical dissolution process without hydrophobic hydration were deduced by extrapolating the linear parts in the high-temperature regions of the respective solubility curves to 25 °C. However, this treatment ought to be applied only to cases in which the solubility data over a sufficiently wide temperature range can clarify the straightening of the solubility curve in the high-temperature region. Thus,

Table 4. Thermodynamic Parameters of Solution at 25 °C for *fac*-Tris(aniono)cobalt(III) of α-Amino Acids and for L-phalaH

No.	Compound	ΔG_s°	ΔH_s°	$T\Delta S_s^\circ$
		kJ mol^{-1}	kJ mol^{-1}	kJ mol^{-1}
11	*fac*-(−)-[Co(D-ala)$_3$]	36.6	7.8	−28.8
12	*fac*-(+)-[Co(D-ala)$_3$]	17.5	0.5	−17.0
13	*fac*-(−)-[Co(D-val)$_3$]	30.8	21.1	−9.7
14	*fac*-(−)-[Co(D-leu)$_3$]	40.1	7.1	−33.0
15	*fac*-(+)-[Co(D-leu)$_3$]	37.8	−0.8	−38.6
16	*fac*-(+)-[Co(L-pro)$_3$]	34.3	13.8	−20.5
17	*fac*-(−)-[Co(L-pro)$_3$]	22.8	5.4	−17.4
18	*fac*-(+)-[Co(L-ser)$_3$]	33.3	27.7	−5.6
19	*fac*-(−)-[Co(L-ser)$_3$]	17.1	20.1	3.0
20	*fac*-(−)-[Co(D-pro)$_3$]	34.4	14.1	−20.3
21	*fac*-(+)-[Co(D-pro)$_3$]	22.8	5.8	−17.0
22	*fac*-(−)-[Co(D-ser)$_3$]	33.8	32.0	−1.8
23	*fac*-(+)-[Co(D-ser)$_3$]	17.2	19.2	2.0
3	*fac*-(−)-[Co(L-ala)$_3$][a)]	17.4	−0.5	−17.9
	L-phalaH	14.4	12.4	−2.0

a) Redetermined in this work.

in this paper the dissolution behavior of *fac*-[Co(amino acidato)$_3$] is discussed on the basis of the thermodynamic parameters of the real dissolution process.

A plot of ΔH_s° against $T\Delta S_s^\circ$ is shown in Fig. 5, where the data for both of the chelates examined in the preceding work[1)] and some amino acids are also plotted. The thermodynamic parameters of solution for glyH, L-leuH, D-alaH, DL-valH, and DL-serH were estimated without any activity correction from the literature values of their solubilities.[5,8)] This plot gives separate correlation lines for the less-soluble chelates, for the more-soluble chelates, and for the amino acids. These correlation lines are expressed by:

$$\Delta H_s^\circ = 0.765 T\Delta S_s^\circ + 29.624 \quad (n = 17, \gamma = 0.965), \qquad (1)$$

$$\Delta H_s^\circ = 0.853 T\Delta S_s^\circ + 17.556 \quad (n = 6, \gamma = 0.964), \qquad (2)$$

and

$$\Delta H_s^\circ = 0.819 T\Delta S_s^\circ + 11.202 \quad (n = 6, \gamma = 0.930), \qquad (3)$$

respectively, where n and γ are the number of samples and the correlation coefficient, respectively.

The above correlation between ΔH_s° and $T\Delta S_s^\circ$ implies that the contribution of $T\Delta S_s^\circ$ to ΔG_s° is superior to the contribution of ΔH_s°. In order to clarify the implication, ΔH_s° is plotted against ΔG_s° in Fig. 6. The solid lines in Fig. 6 indicate the relation between ΔH_s° and ΔG_s° derived by substituting Eqs. 1, 2, and 3 for $\Delta G_s^\circ = \Delta H_s^\circ - T\Delta S_s^\circ$. Within the respective groups, the variation of ΔG_s°, that is, the solubility, is considerably small in contrast to the change of ΔH_s°, and ΔG_s° decreases with increasing ΔH_s°. In other words, the increase in $T\Delta S_s^\circ$ is sufficient to compensate for the in-

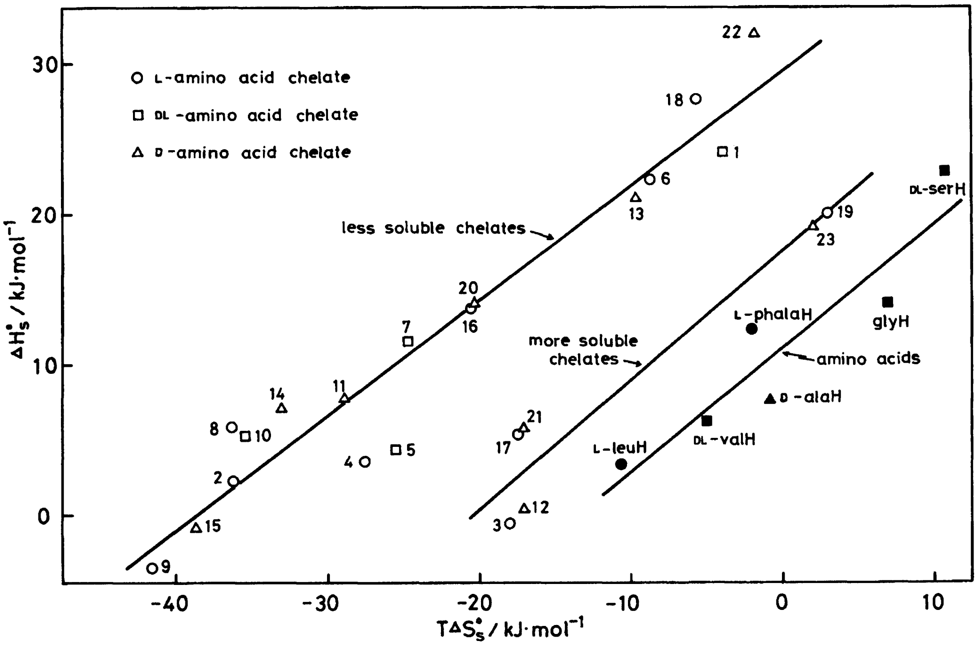

Fig. 5. Compensation relation between ΔH_s° and $T\Delta S_s^\circ$ for *fac*-[Co(α-amino acidato)$_3$] and α-amino acids. The numbers of 11 to 23 indicated beside the symbols correspond to those listed for the respective chelates in Table 4. The numbers of 1 to 10, which correspond to the chelates examined in the preceding work (Ref. 1), are as follows; 1, *fac*-[Co(gly)$_3$]; 2, *fac*-(+)-[Co(L-ala)$_3$]; 3, *fac*-(−)-[Co(L-ala)$_3$]; 4, *fac*-(+)-[Co(L-ambt)$_3$]; 5, *fac*-[Co(DL-ambt)$_3$]; 6, *fac*-(+)-[Co(L-val)$_3$]; 7, *fac*-[Co(DL-nval)$_3$]; 8, *fac*-(+)-[Co(L-leu)$_3$]; 9, *fac*-(−)-[Co(L-leu)$_3$]; 10, *fac*-[Co(DL-nleu)$_3$]. The data for the amino acids other than L-phalaH were estimated from the literature values of the solubilities (Refs. 5 and 8). The solid lines were obtained by the least-squares fit to the three groups composed of the less soluble chelates, the more soluble chelates, and the amino acids.

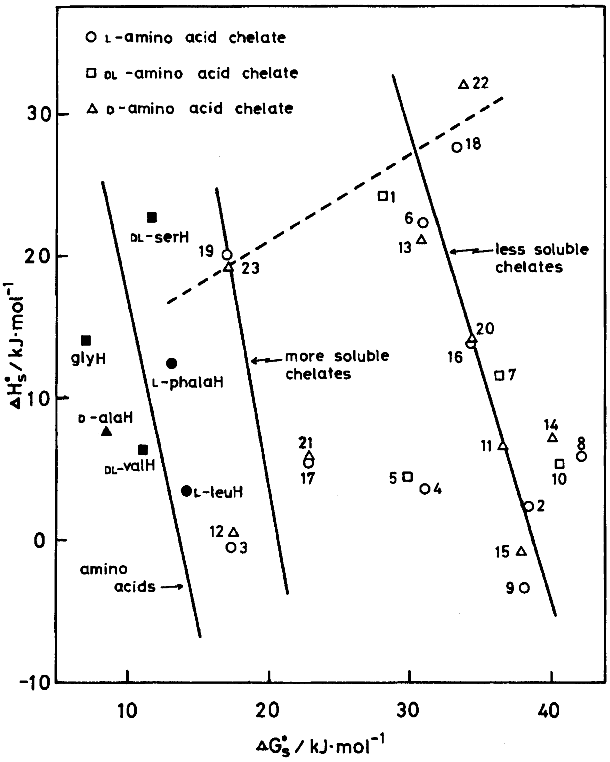

Fig. 6. Contribution of ΔH_s° to ΔG_s° for *fac*-[Co(α-amino acidato)$_3$] and α-amino acids. The solid lines were obtained by substituting the equations of the straight lines in Fig. 5 for $\Delta G_s^\circ = \Delta H_s^\circ - T\Delta S_s^\circ$. The broken line was obtained by applying the least-squares method to the data of the hydrophilic chelates (1, 18, 19, 22, and 23). See the caption to Fig. 5 for numbering.

crease in ΔH_s°, and the excess increase in $T\Delta S_s^\circ$ results in an increase in the solubility.

Figures 5 and 6 also indicate that both ΔH_s° and $T\Delta S_s^\circ$ of hydrophilic *fac*-[Co(gly)$_3$], *fac*-[Co(L-ser)$_3$], and *fac*-[Co(D-ser)$_3$] are larger than those of the other hydrophobic chelates. For the former chelates the correlation between ΔH_s° and ΔG_s°, expressed by

$$\Delta H_s^\circ = 0.607\Delta G_s^\circ + 8.910 \quad (n = 5, \gamma = 0.944), \qquad (4)$$

may be recognized (see the broken line in Fig. 6). It is noteworthy that *fac*-(+)-[Co(L-val)$_3$] and *fac*-(−)-[Co(D-val)$_3$] are close to the broken line. This result suggests that the hydrophobic effect of these chelates of L- and D-valH is fairly small in contrast to the expectation based on the number of carbon atoms in the alkyl side chain of valH.

The thermodynamic parameters of solution for the amino acids give the same conclusion as does *fac*-[Co(amino acidato)$_3$]. This finding demonstrates that an examination of the properties of the amino acid chelates can provide useful information for interpreting the properties of the amino acid residues in proteins and peptides.

For the diastereoisomers of *fac*-[Co(ala)$_3$], *fac*-[Co(pro)$_3$], and *fac*-[Co(ser)$_3$], for example *fac*-(+)-[Co(L-ala)$_3$] and *fac*-(−)-[Co(L-ala)$_3$] (2 and 3 in Figs. 5 and 6), the less-soluble isomers and the more-soluble isomers constitute the separate correlation lines in Figs. 5 and 6. Since both the decrease in ΔH_s° and the increase in $T\Delta S_s^\circ$ contribute to the large solubilities of the more-soluble isomers, the difference in the solubilities of these diastereoisomers is considerably large. On the other hand, the diastereoisomers of *fac*-[Co(leu)$_3$] are placed on the only correlation line comprising the less soluble chelates. Therefore, the compensation relation between ΔH_s° and $T\Delta S_s^\circ$ results in the small difference in the solubilities of the diastereoisomers of *fac*-[Co(leu)$_3$].

In general, the solubilities of antipodes should be identical to each other. As shown in Fig. 1, the antipodes of the (+)- and (−)-isomers of *fac*-[Co(L-amino acidato)$_3$] are the (−)- and (+)-isomers of the corresponding *fac*-[Co(D-amino acidato)$_3$], respectively. The S_m values for *fac*-(−)-[Co(L-ala)$_3$] reported in the preceding paper[1] are considerably smaller than those for *fac*-(+)-[Co(D-ala)$_3$] in Table 1. Since the yield of *fac*-(−)-[Co(L-ala)$_3$] obtained by the preceding procedure was very low, it may be pointed out that the small solubilities reported previously were produced by unsaturation due to an insufficiency of the crystal. Thus, the solubility of *fac*-(−)-[Co(L-ala)$_3$] was redetermined in this work.

In Fig. 7, $\ln X_s$ at 25 °C for the (+)- or (−)-isomer of *fac*-[Co(L-amino acidato)$_3$] is plotted against $\ln X_s$ at 25 °C for the (−)- or (+)-isomer of the corresponding

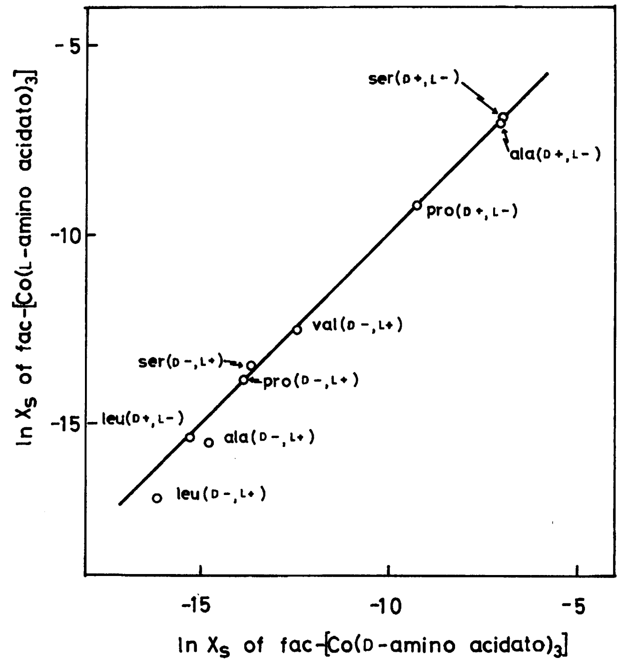

Fig. 7. Relation between $\ln X_s$ at 25 °C for the antipodes of *fac*-[Co(α-amino acidato)$_3$]. For example, leu(D−,L+) denotes the plot of $\ln X_s$ of *fac*-(+)-[Co(L-leu)$_3$] against $\ln X_s$ of *fac*-(−)-[Co(D-leu)$_3$]. The solid line expresses the relation of $\ln X_s(\text{L}) = \ln X_s(\text{D})$.

fac-[Co(D-amino acidato)$_3$]. The solid line in Fig. 7 expresses the relation of $\ln X_s(\mathrm{L}) = \ln X_s(\mathrm{D})$, where L and D in the parentheses denote the $\ln X_s$ values for the L- and D-amino acid chelates, respectively. It may be concluded that the solubility data of the examined antipodes satisfy the relation $\ln X_s(\mathrm{L}) = \ln X_s(\mathrm{D})$.

The author is grateful to Professor T. Murakami for obtaining the CD spectra.

References

1) Y. Yoshimura, *Inorg. Chim. Acta*, **65**, 207 (1993).
2) Y. Yoshimura, *Can. J. Chem.*, **69**, 1388 (1991).
3) R. G. Denning and T. S. Piper, *Inorg. Chem.*, **5**, 1056 (1966).
4) Y. Yoshimura, N. Sato, and M. Kikuchi, *Bull. Chem. Soc. Jpn.*, **59**, 2135 (1986).
5) J. B. Dalton and C. L. A. Schmidt, *J. Biol. Chem.*, **109**, 241 (1935).
6) Y. Yoshimura, *Can. J. Chem.*, **67**, 2108 (1989).
7) M. M. Duke, A. W. Hakin, R. M. McKay, and K. E. Preuss, *Can. J. Chem.*, **72**, 1489 (1994).
8) J. B. Dalton and C. L. A. Schmidt, *J. Biol. Chem.*, **103**, 549 (1933).